GA–A23418

HIGH DENSITY H–MODE DISCHARGES WITH GAS FUELING AND GOOD CONFINEMENT ON DIII–D

by
A.W. LEONARD, T.H. OSBORNE, M.A. MAHDAVI,
M.E. FENSTERMACHER, C.J. LASNIER, T.W. PETRIE,
and J.G. WATKINS

AUGUST 2000

DISCLAIMER

GA–A23418

HIGH DENSITY H–MODE DISCHARGES WITH GAS FUELING AND GOOD CONFINEMENT ON DIII–D

by
A.W. LEONARD, T.H. OSBORNE, M.A. MAHDAVI,
M.E. FENSTERMACHER,* C.J. LASNIER,* T.W. PETRIE,
and J.G. WATKINS†

This is a preprint of a paper presented at the 27th European Physical Society Conference on Controlled Fusion and Plasma Physics, June 12–16, 2000 in Budapest, Hungary and to be published in the *Proceedings.*

*Lawrence Livermore National Laboratory, Livermore, California
†Sandia National Laboratories, Albuquerque, New Mexico

Work supported by
the U.S. Department of Energy under Contract Nos. DE-AC03-99ER54463,
W-7405-ENG-48 and DE-AC04-94AL85000

GA PROJECT 30033
AUGUST 2000

High Density H–mode Discharges with Gas Fueling and Good Confinement on DIII–D

A.W. Leonard,[1] T.H. Osborne,[1] M.A. Mahdavi,[1] M.E. Fenstermacher,[2] C.J. Lasnier,[2] T.W. Petrie,[1] and J.G. Watkins[3]

[1]General Atomics, P.O. Box 85608, San Diego, California 82186-5608
[2]Lawrence Livermore National Laboratory, Livermore, California
[3]Sandia National Laboratories, Albuquerque, New Mexico

H–mode operation at high density is an attractive regime for future reactor-grade tokamaks [1]. High density maximizes fusion power output while the high confinement of H–mode keeps the plasma energy loss below the alpha heating power. One concern though is the energy released due to individual ELMs must be kept small to protect the divertor target from excess ablation. We report on discharges in DIII–D with electron densities as high as 1.45 times the Greenwald density, $n_{GW}(10^{20}m^{-3})=I_p(MA)/[\pi a^2(m)]$, with good confinement, $H_{ITER89P}=1.9$, and ELMs with energy amplitude small enough to protect the divertor. These results were achieved at low triangularity single-null divertor, δ~0.0 with a plasma current of 1.2 MA, q_{95}~3–4, and moderate neutral beam heating power of 2–4 MW. The density was controlled by moderate gas puffing and private flux pumping. A typical discharge is shown in Fig. 1 where upon gas puffing the pedestal density, $n_{e,ped}$, quickly rises to ~$0.8\times n_{GW}$. The confinement initially drops with the gas puff, on a longer timescale the central density rises, peaking the profile and increasing the confinement until an MHD instability terminates the high density and high confinement phase of the discharge. In this report we describe in detail edge pedestal changes and its effect on confinement as the density is increased. We then describe peaking of the density profile that offsets degradation of the pedestal at high density and restores good confinement. Finally we describe the small benign ELMs that result at these high densities.

At high density, DIII–D is in the stiff temperature regime [2] where the central temperature, $T_i(0) \approx T_e(0)$, is proportional to the pedestal temperature, $T_{i,ped} \approx T_{e,ped}$. In this regime the plasma stored energy will be proportional to $P_{e,ped}$, assuming no changes to the density profile shape. Achieving good confinement at high density is then dependent upon maintaining a robust pedestal as density increases. A previous study [2] of the pedestal at this triangularity and divertor configuration in DIII–D showed the pedestal pressure remains constant up to a density of $n_{e,ped}/n_{GW}$=0.7–0.8 before the pedestal begins to degrade. This

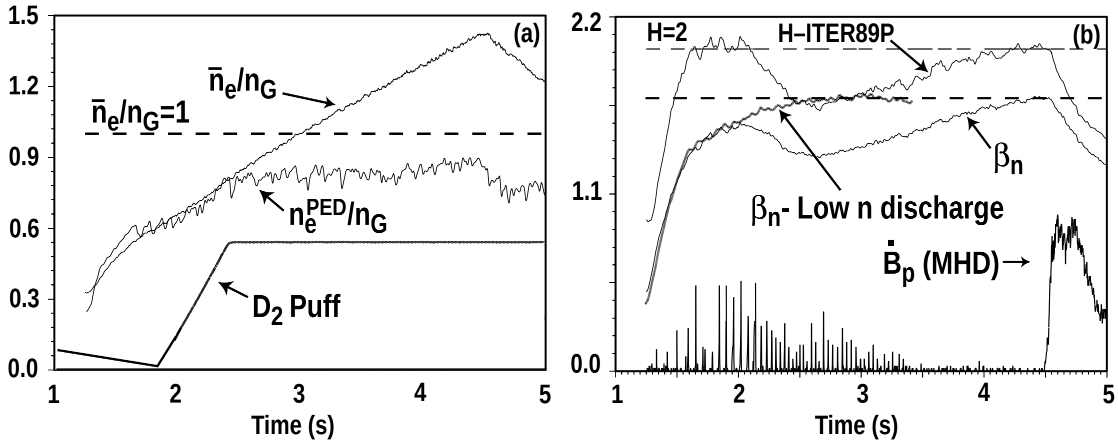

Fig. 1. High density gas puff fueled discharge with good energy confinement. Plasma stored energy, $\beta_n=\beta(\%)aB/I(MA)$, increases as the density profile peaks ($n_e(\rho=0)/n_{e,ped}=2.1$ compared to 1.8 at low density). β_n reaches a level comparable with that of a low density discharge at the same heating power before the density rise is terminated by an MHD event (primaritly m=3, n=2 mode).

threshold corresponds to a line-averaged density of n_e/n_{GW}~0.9, below which the confinement should remain high after the density profile returns to its equilibrium shape. With only a small increase in edge density above this threshold, $n_{e,ped}/n_{GW}$~0.85, $T_{e,ped}$ drops from ~400 eV down to ~200 eV, resulting in a ~40% drop in the pedestal pressure, $P_{e,ped}$. The pedestal degradation results in a similar decrease in stored energy until peaking of the density profile compensates for the degraded pedestal, restoring good confinement.

As long as $T_{e,ped}$ remains >200 eV the edge remains in the Type I ELM regime [3] with a steep H–mode edge density gradient. If the gas puff level is raised too high $T_{e,ped}$ is reduced below 200 eV and a transition to the Type III ELM regime occurs [4]. Type III ELMs are generally characterized by a much smaller edge pressure gradient and poor confinement. In this Type III ELM regime, with excessive gas puffing, the edge and overall density will actually decrease to below that with a lesser gas puff.

The divertor configuration also appears to be important in achieving optimal high density operation. With the divertor strike-point at large major radius, δ~0.0, $T_{e,ped}$ could be reduced to as low as 200 eV before a transition to Type III ELMs, or L–mode occurs. In contrast, at higher divertor triangularity, δ~0.3, a transition to L–mode occurs at a $T_{e,ped}$ above 300 eV. The H–mode threshold is generally lower for a lower triangularity divertor and reducing the toroidal field allowed for lower $T_{e,ped}$ at high divertor triangularity, with the recovery of many aspects of high density operation.

Divertor pumping was found to aid high density operation but appears to be not fundamentally required. No significant difference was found in the Type III or L–mode critical temperatures with or without pumping, even though the gas puff rates required to produce the transition were increased by a factor of 3 or more with pumping. Though many aspects of high density operation were obtained without pumping, steady-state edge H–mode conditions with a large $n_{e,ped}$, and low $T_{e,ped}$, were not achieved. It is not clear, however, whether finer adjustment of the fueling rate could have produced steady state edge conditions without pumping as well.

As mentioned earlier, high confinement at high density is associated with spontaneous peaking of the density profile. This relationship is summarized in Fig. 2. While the pedestal density and temperature profile reach steady state quickly after the onset of gas puffing

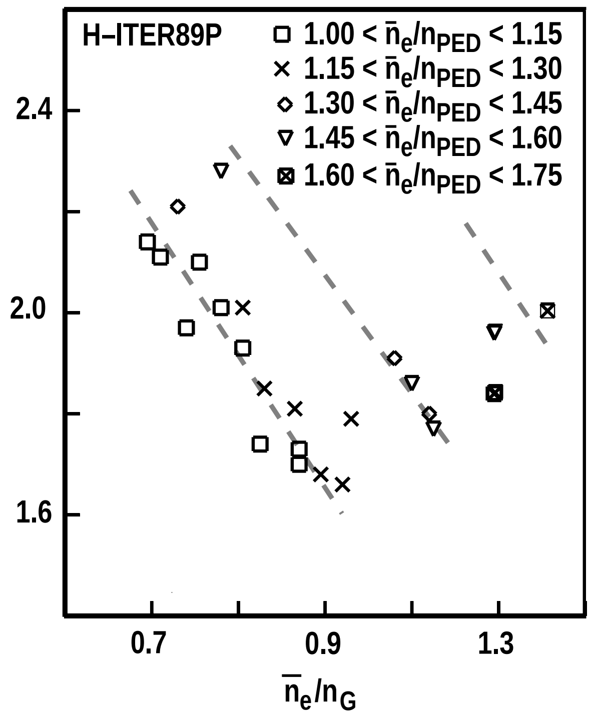

Fig. 2. Obtaining high energy confinement in high density gas puff fueled discharges is accompanied by peaking of the density profile.

(Fig. 1) the central density continues to rise. The nearly linear rise in density is terminated only by the onset of MHD instability. The density peaking appears to be enhanced at low heating power which suggests the neoclassical Ware pinch with an inward flux given by $\Gamma_W \approx \varepsilon^{1/2} n E_T / B_p \sim n/T^{3/2}$. Particle transport in these discharges was determined by measuring the evolution of the helium profile with CER after a brief helium gas injection. Assuming the helium transport is similar to the main ions, the central density rise is due to both a reduction in particle diffusivity and a strong inward pinch. Comparing transport just after the L-H transition to that midway through the density rise, the particle diffusivity is found to decrease by about a factor of 2 from 0.28 m^2/s to 0.14 m^2/s outside of ρ=0.4. A strong inward pinch also develops from slightly outward just after the L-H transition to an inward velocity of ~ 0.5 m/s also outside of ρ=0.4. This inward pinch is almost a factor of 10 larger than the neoclassical value calculated from the measured profiles.

The density and stored energy rise for discharges which reach $n_e/n_{GW} > 1.1$ is terminated by the onset of MHD modes. Typically a series of modes in the region between the q=1 and q=3/2 surface are observed. This region, near ρ=0.4–0.5, has increasing pressure gradient as a result of the peaking of the density profile leading to a more peaked bootstrap current profile. The increased current density in this region, due to the additional bootstrap current, tends to increase the instability of the tearing mode. It is under these conditions that the neoclassical tearing mode (NTM) can be triggered by a seed island, perhaps from an ideal mode or some other instability. A large mode then results with the subsequent loss of confinement, perhaps a consequence of the overlap of adjacent modes.

An additional benefit of high density operation is the reduction of the size of ELMs. The very large transient heat flux due to individual ELMs can lead to divertor surface ablation and unacceptable target plate erosion [5]. A previous multi-machine study [6] of low to moderate density H–mode found that the energy released at each ELM was approximately 1/3 of the pedestal electron energy. The pedestal energy is defined as the pedestal temperature times the plasma volume. The conclusion of this study was that the high pedestal values desired for good confinement in future large tokamaks would lead to ELMs a factor of 5 too large for acceptable divertor target erosion.

To determine the relationship between ELMs and $P_{e,ped}$ at higher density, the energy loss due to individual ELMs was measured during the density scans described above. The ELM energy is determined by evaluating the plasma stored energy with a fast magnetic equilibrium analysis 1.5 ms before and after each ELM, with the ELM time determined from the fast rise in divertor H_α. In addition, discharges with increased upper triangularity, from δ~0.0 to δ~0.36, but with the same lower divertor configuration, were included in the ELM analysis to separate n_e and T_e dependence of the ELM energy. The higher triangularity discharges generally display a higher $P_{e,ped}$ leading to a higher $T_{e,ped}$ at the same $n_{e,ped}$. Plotted in Fig. 3 is the normalized ELM energy, ΔW_n, which is the ELM energy divided by $P_{e,ped}$ times the plasma volume. For low δ the relative ELM energy continually decreases as the density increases. For higher δ the ELM energy does not decrease until $n_{e,ped}/n_{GW} \geq 0.65$. Because $P_{e,ped}$ remains nearly constant up to $n_{e,ped}/n_{GW} \leq 0.75$, for both low and high δ, any reduction in ΔW_n represents an absolute reduction in ELM energy. Above this level the ELM energy decreases faster than $P_{e,ped}$, quickly dropping to within the measurement uncertainty of ~5 kJ. In Fig. 3(b), ΔW_n is plotted versus $T_{e,ped}$. The ELM energy drops for $T_{e,ped}$ below about 600 eV. Whatever process is reducing the ELM size as density increases, it appears to be more correlated with T_e than n_e.

Profiles of edge n_e and T_e collected from Thomson scattering just before and just after ELMs highlight other details of the ELM process. These profiles show that at low density both the n_e and T_e profiles are perturbed by the ELM up to 4–5 cm inside the separatrix at the midplane. $P_{e,ped}$ drops nearly a factor of 2 after the ELM in this case. At high density the relative perturbation to n_e is similar to the low density case, however, the perturbation to T_e in the edge becomes almost negligible. The large perturbation to T_e at low density may be due to conductive transport where stochastic field lines during the ELM allow heat to flow across the separatrix. At high density the ELM transport may become convective where particles are carried across the steep density gradient at the edge with little change to T_e. Changes to the ELM instability at high density are also seen by B-dot Mirnov probes; the magnetic fluctuations during an ELM drop a factor of 5–10 compared to low density. This may be a

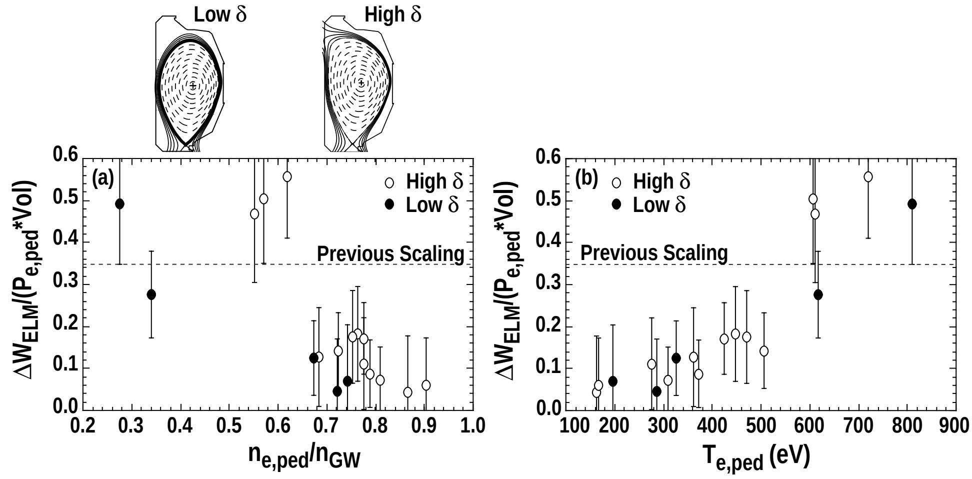

Fig. 3. ΔW_n, the ELM energy normalized by the pedestal electron energy, plotted as a function of (a) the pedestal density, and (b) the pedestal electron temperature. The low and high triangularity configurations are also shown.

result of the ELM instability growth rate and/or the mode number of the ELM increasing. A higher mode number will result in the magnetic perturbation due to the ELM to be more localized in the plasma edge.

Discharges on DIII–D demonstrate that it is possible to exceed the Greenwald density with good energy confinement and small ELMs. For line-averaged densities of ~90% of n_{GW}, good confinement relies upon maintaining a robust pedestal. At high density, and high collisionality, the edge bootstrap current would be expected to decrease significantly affecting the edge stability. This could affect both the pedestal pressure gradient and the mode number of the most unstable ELM instability. In the DIII–D results there appears to be a window where the edge pressure is decreased only slightly and the ELMs are significantly smaller. Other processes that may be playing an equal role include finite resistivity in the pedestal and edge effects such as neutral fueling and divertor detachment. Further analysis and modeling is needed to interpret this data and predict results for future larger tokamaks.

Achievement of higher density, $n_e/n_{GW} \geq 1.1$ might require a peaking of the density profile. If the observed density peaking is due to the neoclassical Ware pinch then the scaling of this effect to a large tokamak is unfavorable. Using ITER-89P scaling for both particle and energy confinement, an ITER sized device would be expected to have a density peaking due to neoclassical effects only 2% of that observed on DIII–D. However, the peaking on DIII–D is much larger than would be expected from neocassical effects, and a pinch might also result from other effects such as turbulent transport where the electron bounce frequency is high compared to the mode frequency. This would allow for the possibility of density peaking in future large devices.

Work supported by U.S. Department of Energy under Contracts DE-AC03-99ER54463, W-7405-ENG-48, and DE-AC04-94AL85000.

[1] ITER Physics Basis Editors, *et al*. Nucl. Fusion **39**, 2137 (1999).
[2] T.H. Osborne, J.R. Ferron, M.E. Fenstermacher, *et al*., "The Effect of Plasma Shape on H–mode Pedestal Characteristics," accepted for publication in Plasma Phys. and Contr. Fusion.
[3] H. Zohm, Plasma Phys. Control. Fusion **38**, 105 (1996).
[4] O. Pogutse, *et al*., Proc. 26th EPS Conf. on Controlled Fusion and Plasma Physics, Maastricht, The Netherlands, Vol **23J**, p. 249 (1999).
[5] H.D. Pacher, "E9. Disruption and ELM Erosion," Appendix E9, Section 1.7 (Divertor), ITER Design Description Document, ITER No. "G 17 DDD 1 96-08-21 W2.1," August 1996.
[6] A.W. Leonard, A. Herrmann, K. Itami, *et al*., J Nucl. Mater. **266-269** 109 (1999).